Published in final edited form as:
*IEEE Trans Biomed Eng*. 2011 June ; 58(6): 1706–1714. doi:10.1109/TBME.2011.2111419.

# Shear elastic modulus estimation from indentation and SDUV on gelatin phantoms

**Carolina Amador**[*] **[Student Member, IEEE]**,
Ultrasound Research Laboratory, Department of Physiology and Biomedical Engineering, Mayo Clinic College of Medicine, Rochester, MN

**Matthew W. Urban[Member, IEEE]**,
Ultrasound Research Laboratory, Department of Physiology and Biomedical Engineering, Mayo Clinic College of Medicine, Rochester, MN

**Shigao Chen[Member, IEEE]**,
Ultrasound Research Laboratory, Department of Physiology and Biomedical Engineering, Mayo Clinic College of Medicine, Rochester, MN

**Qingshan Chen**,
Biomechanics Laboratory, Division of Orthopedic Research, Mayo Clinic College of Medicine, Rochester, MN

**Kai-Nan An**, and
Biomechanics Laboratory, Division of Orthopedic Research, Mayo Clinic College of Medicine, Rochester, MN

**James F. Greenleaf[Life Fellow, IEEE]**
Ultrasound Research Laboratory, Department of Physiology and Biomedical Engineering, Mayo Clinic College of Medicine, Rochester, MN

Matthew W. Urban: urban.mathew@mayo.edu; Shigao Chen: chen.shigao@mayo.edu; Qingshan Chen: chen.qingshan@mayo.edu; Kai-Nan An: an.kainan@mayo.edu; James F. Greenleaf: jfg@mayo.edu

## Abstract

Tissue mechanical properties such as elasticity are linked to tissue pathology state. Several groups have proposed shear wave propagation speed to quantify tissue mechanical properties. It is well known that biological tissues are viscoelastic materials; therefore velocity dispersion resulting from material viscoelasticity is expected. A method called Shearwave Dispersion Ultrasound Vibrometry (SDUV) can be used to quantify tissue viscoelasticity by measuring dispersion of shear wave propagation speed. However, there is not a gold standard method for validation. In this study we present an independent validation method of shear elastic modulus estimation by SDUV in 3 gelatin phantoms of differing stiffness. In addition, the indentation measurements are compared to estimates of elasticity derived from shear wave group velocities. The shear elastic moduli from indentation were 1.16, 3.40 and 5.6 kPa for a 7, 10 and 15% gelatin phantom respectively. SDUV measurements were 1.61, 3.57 and 5.37 kPa for the gelatin phantoms respectively. Shear elastic moduli derived from shear wave group velocities were 1.78, 5.2 and 7.18 kPa for the gelatin phantoms respectively. The shear elastic modulus estimated from the SDUV, matched the elastic modulus measured by indentation. On the other hand, shear elastic modulus estimated by group velocity did not agree with indentation test estimations. These results suggest that shear elastic modulus estimation by group velocity will be bias when the medium



[*]amadorcarrascal.carolina@mayo.edu.

being investigated is dispersive. Therefore a rheological model should be used in order to estimate mechanical properties of viscoelastic materials.

**Index Terms**

Indentation; SDUV; elasticity

## I. Introduction

Noninvasive measurement of tissue mechanical properties as an estimator for tissue pathology is an emerging field of medical imaging [1–8]. In principle, all elasticity imaging methods introduce mechanical excitation to tissue and then monitor the tissue response with conventional imaging methods. The first proposed elasticity imaging methods either excite tissue externally, as in ultrasound elastography [9], or use focused ultrasound to produce acoustic radiation force to push tissue as in acoustic radiation force impulse (ARFI) imaging [3]. While elastography and ARFI are useful approaches, they do not provide a quantitative measure of tissue stiffness; both methods typically form a 2D image providing a relative map of tissue stiffness. Shear wave propagation speed methods, such as magnetic resonance elastography (MRE) [1], shear wave elasticity imaging (SWEI) [7], Transient elastography (TE) [2] and supersonic shear imaging (SSI) [10], have been proposed to quantify tissue mechanical properties. Most of these methods consider a pure elastic medium to describe the tissue mechanical properties, therefore only tissue elasticity is quantified.

Shear wave speed, $c_s$, in a pure elastic medium is related to the shear modulus, $G$, and density, $\rho$, by

$$c_s = \sqrt{\frac{G}{\rho}} \tag{1}$$

The wave speed in a given medium can be defined by the velocity of a single frequency component (phase velocity) or the velocity of the wave packet (group velocity). In a non-dispersive medium, phase velocity is the same as group velocity. In such circumstance, the wave velocity is independent of frequency. In contrast, in a dispersive medium, the wave speed is dependent on frequency; therefore phase velocity is not the same as group velocity in a dispersive medium. Dispersion can be caused by both tissue geometry and material properties.

It has been established that soft biological tissues exhibit a combination of elastic and viscous behavior [11]. A material subject to periodic oscillations exhibits a complex modulus $M(\omega)$ described by [12]

$$M(\omega) = M_1(\omega) + jM_2(\omega) \tag{2}$$

where the real part $M_1(\omega)$ is the elastic or storage modulus, and the imaginary part $M_2(\omega)$ is the loss or viscous modulus. The most common rheological models are the Voigt and the Maxwell model. The Voigt model has been shown to be appropriate for describing viscoelastic properties of tissue in the low frequency range (50–500 Hz) [13–16]. The

complex shear modulus for the Voigt model is given by $M_1(\omega) = \mu_1$ and $M_2(\omega) = \omega\mu_2$, where $\mu_1$ is shear elastic modulus and $\mu_2$ is viscosity [13].

A few elasticity imaging methods take advantage of the dispersive nature of soft tissue and can quantitatively solve for both tissue elasticity and viscosity [10, 17–21]. Even though sonoelastography [8] and supersonic shear imaging (SSI) [10] can provide maps of shear modulus and viscosity, specialized hardware is necessary to implement both methods.

A method called Shearwave Dispersion Ultrasound Vibrometry (SDUV) can be used to quantify both tissue shear elasticity and viscosity by evaluating dispersion of shear wave propagation speed over a certain bandwidth [20, 22]. It is desirable to have an inexpensive, reproducible tool to validate SDUV measurements. Mechanical testing is usually regarded as the gold standard method, but mechanical testing devices are usually very expensive.

Chen, *et al.*, have reported a quantitative model for a sphere vibrated by two ultrasound beams in a homogeneous viscoelastic medium [22]. In this study, a Doppler laser vibrometer was used to measure the mechanical frequency response of the sphere. Although this method can estimate material properties in an independent manner, its main disadvantage is that the medium around the target must be optically clear. To overcome this problem, a single element ultrasound transducer can be used to measure the sphere time-domain response [23, 24], which was then fit using a model to obtain estimates of the shear elasticity and viscosity. However, these methods are not suitable for tissue mechanical properties characterization since a sphere must be embedded within a homogeneous tissue. Therefore, a more comprehensive study is needed to validate SDUV.

Several methods to measure tissue mechanical properties such as stress-relaxation, quasi-static and dynamic test have been used on biological tissues [11]. Mechanical tests had been used to evaluate the accuracy of elasticity methods such as MRE, ARFI and TE. MRE measurements have been compared to compression tests and dynamic tests on tissue like gelatin phantoms of varying elasticity [25, 26]. An integrated indentation and ARFI imaging has been used to characterize soft tissue stiffness [27]. TE measurements have been compared to tensile tests and dynamic test on a tissue like polymers [28, 29]. Cross-validation between MRE and ultrasound-based transient elastography had been made in homogeneous tissue mimicking phantoms [30, 31]. Dynamic tests allow estimation of the change in tissue property parameters versus frequency, but the material needs to be characterized one frequency at a time. Quasi-static methods include compression tests, tensile tests and indentation tests. Compared to the others, indentation tests have been widely used to assess the mechanical properties of tissues. Their main advantage is that they can be applied both *ex vivo* and *in vivo* [11, 32–40]. The indentation test is considered a gold standard test to assess elastic mechanical properties. Furthermore, it is attractive because of its widespread use and ease of implementation, with its only requirement is to have a surface for indenter contact application.

The purpose of this study is to validate linearity and phase velocity assumptions of SDUV estimations of shear elastic modulus with quasi-static indentation measurements of elastic modulus on gelatin phantoms of differing stiffness. In addition, the indentation measurements are compared to estimates of elasticity derived from shear wave group velocities.

# II. Methods

## A. Indentation test

Soft tissue indentation based on a Hayes model [41] was used in this study. Fig. 1 illustrates a lateral infinite isotropic elastic material with a finite thickness resting on a rigid half-space. The material deforms under the action of a rigid axisymmetric indenter pressed normal to the surface by an axial force $F$.

Shear tractions between indenter and material are assumed negligible and the material is assumed to adhere to the half-space rigid surface. For a flat-end cylindrical indenter, the effective shear elastic modulus $G$ is:

$$G=\frac{(1-\nu)}{4a\kappa(\nu, a/h)}\cdot\frac{F}{\delta} \tag{3}$$

where $v$ is the Poisson ratio, $F$ is the indentation force, $\Delta$ is the indentation depth, $a$ is the indenter radius, $h$ is the material thickness and $\kappa$ is a geometry factor. Values of $\kappa$ for a range of $a/h$ and $v$ have been estimated by Hayes, *et al* [41].

## B. Principles of SDUV

Shearwave Dispersion Ultrasound Vibrometry (SDUV) applies a focused ultrasound beam to generate harmonic shear waves or impulse shear waves that propagate outward from the vibration center [19, 20]. Chen, *et al*., originally reported using modulated ultrasound to create harmonic shear waves to characterize the viscoelastic properties of gelatin phantoms using shear wave dispersion [19, 20]. A limitation of this method was that the modulation frequency had to be changed multiple times to evaluate the dispersion over a significant bandwidth. This method was advanced to make faster measurements by transmitting repeated tonebursts of ultrasound [20]. A single toneburst could be used to generate shear wave dispersion but the signal-to-noise ratio at high frequencies may be poor. Although repeated tonebursts require more acquisition time compared to a single toneburst, the advantage of using repeated tonebursts is that shear waves are created that have motion amplitudes with high signal-to-noise ratio at harmonics of the repetition frequency [20, 42].

For an isotropic, viscoelastic, homogenous material modeled using the Voigt model the shear wave propagation speed, $c_s$, depends on the frequency of shear wave, $\omega_s$ [13]

$$c_s(\omega_s)=\sqrt{\frac{2\left(\mu_1^2+\omega_s^2\mu_2^2\right)}{\rho\left(\mu_1+\sqrt{\mu_1^2+\omega_s^2\mu_2^2}\right)}} \tag{4}$$

where $\rho$, $\mu_1$ and $\mu_2$ are the density, shear elastic modulus and viscosity of the medium, respectively.

The shear wave speed is estimated from its phase measured at least at 2 locations separated by $\Delta r$ along its traveling path:

$$c_s(\omega_s)=\omega_s\Delta r/\Delta\varphi_s \tag{5}$$

where $\Delta\varphi_s = \varphi_1 - \varphi_2$ is the phase change over the traveled distance $\Delta r$. Generally, a regression is made on the phase versus distance over an extended region in order to improve wave speed estimation.

The shear wave speed is then estimated with (5). Dispersion measurements at fundamental frequency of 50 Hz and its harmonics of 100 Hz, 150 Hz, 200 Hz, etc. are fit by (4) to solve for shear elastic modulus and viscosity.

## III. Experiments

### A. Gelatin phantom characterization

Three sets of gelatin phantoms were made to compare shear elastic modulus values from indentation tests and SDUV. Gelatin phantoms were made using 300 Bloom gelatin (Sigma-Aldrich, St. Louis, MO) and glycerol (Sigma-Aldrich, St. Louis, MO) with a concentration of 7, 10, and 15% by volume to achieve different values of the shear elastic modulus. A preservative of potassium sorbate (Sigma-Aldrich, St. Louis, MO) was added with a concentration of 7, 10, and 15% by volume. Cellulose particles (Sigma-Aldrich, St. Louis, MO) with size 20 μm were also added with a concentration of 0.5% by volume to provide adequate ultrasonic scattering.

To evaluate the suitability of Hayes' model, two different samples (cylindrical shape) thicknesses were used. Similarly, the impact of sample diameter was evaluated by using three different sample diameters (four samples of each type) and two flat-end cylindrical indenter sizes, a 3 mm indenter diameter and a 2 mm indenter diameter. Table I summarizes the sample characterization.

Additionally, a block of gelatin (15 × 15 × 4 cm) was made from the same batch of each gelatin solution preparation for use in SDUV experiments.

### B. Indentation test

Quasi-static unconfined uniaxial indentation experiments were performed using a mechanical testing machine (Enduratec, ElectroForce® 3200). A 50 gram load cell was used to record load as the flat-end cylindrical indenter was moved at a rate of 0.1 mm/sec. The sampling frequency was 20 kHz. The noise floor of the system was about 0.15 mN. The linear region of the force-displacement curve was defined as described by Zhai, *et al.,* [27]. The absolute difference from the raw data and the fit was calculated. A threshold equal to 3 times the system's floor noise was set. A data window of approximately 20 samples (5% of indenter diameter) was linearly fit. The data window was increased until the absolute difference or error was just below the threshold. Each sample was compressed four times.

### C. SDUV

Fig. 2 illustrates the experimental setup. The 'Push Transducer' (custom made with piezo crystals from Boston Piezo-Optics, Inc., Bellingham, MA) has a diameter of 44 mm, a center frequency of 3 MHz and a focal length of 70 mm. Shear waves generated at the transducer focal point propagate through gelatin phantom and vibration was detected by a single element transducer (Harisonic 13-0508-R, Staveley Sensors Inc.) with a diameter of 12.7 mm, a center frequency of 5 MHz and a 50 mm focus length ('Detect Transducer'). The 'Push Transducer' and 'Detect Transducer' were aligned confocally with a pulse echo technique using a small sphere as a point target. The force was localized 5 mm deep into the gelatin phantom surface.

The pulse repetition frequency of the push tonebursts was 50 Hz and the toneburst length was 300 μs. The propagation of the shear wave was tracked by the single element transducer

in pulse-echo mode over a lateral range of 10 mm. The pulse repetition frequency of the 'Detect Transducer' was 1.6 kHz for the 7% and 10%. Because the 15% gelatin phantom was expected to be stiffer, thus shear waves travel faster, compared to the 7% and 10% gelatin phantoms, the pulse repetition frequency of the 'Detect transducer' for the 15% gelatin phantom was 3.2 kHz.

The ultrasound echoes were digitized at 100 MHz and processed by the cross-spectrum analysis previously described [43] to estimate the shear phase gradient. The shear wave propagation speed was calculated by (5) and dispersion measurements from 50 to 400 Hz were fit by (4) to solve for shear elastic modulus and viscosity. The group velocity for each phantom was calculated by evaluating the time shifts in the shear waves versus position and using

$$c_g = \Delta r / \Delta t \tag{6}$$

where $c_g$ is the group velocity, and $\Delta t$ is the time shift measured over a distance $\Delta r$.

During each experiment, the single element transducer was moved by 1 mm intervals 11 times on *y*-axis (refer to Fig. 2). This acquisition sequence was repeated 4 times in each of the regions of interest (ROI). Additionally, SDUV measurements were repeated at 4 different regions.

## IV. Results

### A. Indentation test

The force-displacement raw data for one sample (Sample type 1, refer to Table I) of 7%, 10% and 15% gel phantom with a 2 mm indenter diameter is shown in Figure 3.

All three phantom samples showed a linear response up to approximately 1 mm compression. The maximum force for each linear region was 9 mN, 40 mN and 63 mN for 7, 10 and 15% phantoms respectively.

Table II shows the influence of sample thickness and sample diameter on the Hayes model for the 7%, 10% and 15% gelatin phantoms. The sample thickness was approximately 5.3, 8, 11.3 and 17 times the indenter radii. Similarly, the sample diameter was approximately 9.2, 13.8, 23.3 and 35 times the indenter radii. Because the geometry factor $\kappa$ is not very sensitive to Poisson's ratio $v$ from 0.45 to 0.5 for $a/h$ ratio range from 0.05 to 0.20, the Poisson's ratio $v$ was set to 0.475.

### B. SDUV

The displacement amplitude estimates over 50 ms for 7% gelatin phantom are shown in Figure 4 and as calculated by the cross-spectrum method [43]. The peak displacement amplitude was approximately 18 μm, 16 μm and 12 μm at 4, 6 and 8 mm away from the vibration center.

The magnitude spectra of the velocity signal for the 7%, 10% and 15% gelatin phantoms over 200 ms are shown in Figure 5. The frequency at which the amplitude is highest, or the center frequency of broadband signal, is denoted as $\omega_p$. The center frequencies of the SDUV response, from 0 ms to 200 ms, were 100 Hz for 7% phantom, 350 Hz for 10% phantom and 100 Hz for the 15% phantom. The group velocity, is described by Morse and Ingard as the

"velocity of progress of the 'center of gravity' of a group of waves that differ somewhat in frequency [44]". The center of gravity was calculated by [45]

$$\omega_c = \sum \omega \cdot |V(\omega)|^2 / \sum |V(\omega)|^2 \tag{7}$$

where $V(\omega)$ is the complex spectrum of the velocity signal and $\omega$ is the frequency. The center of gravity of the magnitude spectrum of the velocity signal for each gelatin phantom was 200, 350 and 250 Hz for the 7, 10 and 15% gelatin phantoms.

Figure 6 shows the distance from the vibration center versus time shift for 7%, 10% and 15% gel phantoms over 5 mm. The time shifts were calculated by cross-correlation method [46]. The solids lines are linear regression for the time shifts. The group velocity was calculated from (6).

The group velocity (slope of solid lines in Fig. 6) for each gelatin phantom was 1.33, 2.35 and 3.15 m/s for 7, 10 and 15% respectively. By assuming a non-dispersive medium, in other words, by setting $\mu_2 = 0$ in (4), and also assuming a linear elastic material, where group velocity is same as the phase velocity for all frequencies, the shear elastic modulus by (1) for the 7, 10 and 15% gelatin phantom was 1.77, 5.52 and 9.92 kPa respectively.

The phase of shear waves at frequencies 50 to 400 Hz was estimated by Kalman filter [47]. Figure 7 illustrates the phase of shear wave at frequencies 100 to 400 Hz for the 7% gel phantom. There is a linear relation between shear wave phase and propagation distance. The solid lines are linear regressions for the phase estimates. The coefficients of determination, $R^2$, of the linear regressions were greater than 0.95, 0.97 and 0.96 for the 7%, 10% and 15% gelatin phantom respectively. This indicates that the linear assumption of (5) is appropriate.

Figure 8 shows shear wave propagation speed as a function of frequency.

The symbols represent the mean shear wave speed of four repetitions for each gelatin phantom. Error bars represent the standard deviation of the measured shear wave speed at each particular frequency four times. The solid lines are the least mean square (LMS) fits from (4) that give a shear elastic modulus of $\mu_1$ = 1.61, 3.30 and 5.37 kPa and viscosity of $\mu_2$ = 0.85, 1.43 and 2.14 Pa·s for 7%, 10% and 15% gelatin phantoms, respectively. The median absolute error, that is, the median of the absolute difference between the Voigt model fit and experimental data, was 0.09, 0.14 and 0.23 m/s for 7, 10 and 15% gelatin phantom respectively.

## V. Discussion

The use of Hayes' model is suitable for describing small deformation indentation on lateral infinite isotropic elastic media. Even though this model takes the sample thickness into account, it is important to satisfy its assumed boundary conditions. Shear elastic modulus was slightly underestimated when the sample diameter was decreased, particularly on the softer phantom. This is caused by the violation of the assumption of lateral infinite geometry. Not surprisingly, there was not a significant variation of shear elastic moduli for different sample thickness (Refer to Table 2) for the 7% and 10% gelatin phantom. However, shear elastic modulus was slightly different for the 15% gelatin phantom for different sample thickness. These observations agree with FEM simulations described by Zhai *et al* [27], suggesting that a sample with 5 kPa of Young's modulus is large enough when its thickness and diameter are over 15 times of the indenter radii. Therefore, the shear

elastic modulus for the 7, 10 and 15 gelatin phantoms were 1.16, 3.40 and 5.60 kPa respectively (refer to Table II). However, a more suitable model should include both sample thickness and sample diameter in consideration.

The peak displacement amplitude estimated by SDUV was approximately 18 μm, which is considered a small displacement and therefore within a linear region of a force-displacement curve. Tissue response to a harmonic excitation using different voltage amplitudes on the 'Push transducer' has shown a fairly independent relationship between shear wave speed and excitation voltage, which is equivalent to a linear relationship between force and displacement [48]. Similarly, the force-displacement curve from the indentation experiments was linear for up to 1 mm. Although force-displacement curves of gelatin phantoms were nonlinear for large displacements (larger than 1 mm), indentation can be used to assess elastic components of mechanical properties of viscoelastic materials under small deformation.

The phase estimates at high frequencies showed more variation compared to lower frequencies (refer to Fig. 7). This was consistent in all 3 phantoms. Because the displacement amplitude is decreased at high frequencies, the error of the phase estimates is expected to increase at high frequencies [49]. However, the coefficients of determination, $R^2$, of the linear regressions were high in all 3 phantoms.

Table III shows a comparison between group velocity ($c_g$), phase velocity evaluated at center of gravity ($c_s(\omega_c)$)and phase velocity evaluated at center frequency ($c_s(\omega_p)$). Both phase velocities calculations were close to group velocities for the 7 and 10% gelatin phantom. The magnitude spectrum of the velocity signal for the 15% phantom (Refer to Fig. 5) was broader compared to the other phantoms. This could be a reason why the group velocity for the 15% gelatin phantom was rather different than the phase velocities. In theory, the group velocity should be identical or close to the phase velocity $c_s$ evaluated at $\omega_c$.

The shear wave speed versus frequency results in Figure 8 fits well with the Voigt model, particularly for the softer phantom. Stiffer phantoms seem to have peaks at certain frequencies that deviate from the ideal Voigt model, however the absolute error between the Voigt model fit and experimental data was not significantly large. Shear wave estimation may be affected by tissue geometry depending on the type of wave that is being excited. For instance, mathematical models for shear wave dispersion of anti-symmetric Lamb and Rayleigh suggest that shear wave speed is affected by material thickness mostly at lower frequencies when the material thickness is larger than one to two wavelengths of the wave [50]. Although the largest wavelength, about 42 mm for the 15% gelatin phantom at 50 Hz, was approximately equal to the phantom thickness, substantial errors for measurement of the shear wave speed related to phantom thickness are not expected. SDUV generates pure shear waves, that is, a shear wave propagating in an infinite medium, therefore SDUV assumes there are no reflections from boundaries. In addition, the phase gradient in equation (5) assumes that there is only one wave traveling one direction. Therefore, reflections from the surface may cause variations in the phase and cause errors in the speed measurements.

The SDUV method assumes a viscoelastic material by implying a complex shear elastic modulus. The compression rate for the indentation test was 0.1 mm/sec and each gelatin showed a linear response up to 1 mm compression, therefore the excitation frequency for indentation test was approximately 0.1 Hz. Because the excitation frequency from the indentation test is close to zero, the shear elastic modulus estimation by indentation test should be the same or close to the real component of the shear complex modulus on the Voigt model.

Figure 9 provides a summary of the shear elastic modulus estimated from group velocity (linear elastic medium), phase velocity (viscoelastic medium, Voigt model) and indentation test. Error bars represent the standard deviation of the measured shear elastic modulus for each particular phantom at four different locations.

The shear elastic modulus estimated from group velocity measurements can definitively differentiate the three phantoms. However, these values do not agree well with both the indentation experiment results and phase velocity results, especially when the phantom is stiffer. This disagreement could be attributed to the fact that gelatin phantoms are dispersive [13, 16, 19]; therefore the wave speed is dependent on frequency. Shear elastic modulus estimation from the indentation test and phase velocity for the 7% phantom were slightly different. This could be due to inhomogeneities on gelatin samples. The cellulose component, introduced for ultrasound scattering, did tend to settle down in the sample molds while the gelatin was liquid. Because the 7% gelatin is less viscous, the cellulose distribution was probably different compared to the other phantoms.

A linear correlation comparing shear elastic modulus from indentation test with group velocity and SDUV phase velocity is shown in Figure 10. The correlation coefficients were 0.98 for the group velocity and 0.99 for the SDUV phase velocity method. Although the correlation coefficients are similar and large, most likely because the number of gelatin phantoms is small, the shear elastic modulus correlation between SDUV phase velocity method and indentation test is closer to the ideal correlation (continuos line on Fig. 10). On the other hand, the shear elastic modulus correlation between group velocity and indentation test seem considerably different from the ideal correlation, suggesting that shear elastic modulus estimation by group velocity will be bias when the medium being investigated is dispersive. Therefore a rheological model should be used in order to estimate mechanical properties of viscoelastic materials. Because tissues are more viscous than these phantoms [16, 19, 20], this would be the case for tissues as well. This study shows acceptable agreement of shear elastic moduli estimates from SDUV phase velocity method and indentation test on gelatin phantoms.

## VI. Conclusion

In this paper, we present an independent validation method of elastic modulus estimation by SDUV in gelatin phantoms. The shear elastic modulus, estimated from the SDUV phase velocity method, matched the elastic modulus measured by the indentation method. The shear elastic modulus estimated by group velocity did not agree with indentation test estimations. These results suggest that a rheological model for linear viscoelastic material must be used to estimate elastic modulus on gelatin phantoms and soft tissue.

## Acknowledgments

This work was supported in part by Grant number DK082408 from National Institutes of Health.

## References

1. Muthupillai R, Lamos DJ, Rossman PJ, Greenleaf JF, Manduca A, Ehman RL. Magnetic resonance elastography by direct visualization of acoustic strain waves. Science. 1995; 269:1854–1857. [PubMed: 7569924]
2. Sandrin L, Fourquet B, Hasquenoph JM, Yon S, Fournier C, Mal F, Christidis C, Ziol M, Poulet B, Kazemi F, Beaugrand M, Palau R. Transient elastography: A new noninvasive method for assessment of hepatic fibrosis. Ultrasound Med Biol. 2003; 29:1705–1713. [PubMed: 14698338]
3. Nightingale K. Shear-wave generation using acoustic radiation force: in vivo and ex vivo results. Ultrasound in Medicine & Biology. 2003; 29:1715–1723. [PubMed: 14698339]

4. Catheline S, Thomas JL, Wu F, Fink MA. Diffraction field of a low frequency vibrator in soft tissues using transient elastography. IEEE Transactions on Ultrasonics Ferroelectrics and Frequency Control. 1999; 46:1013–1019.
5. Catheline S, Wu Fo, Fink M. A solution to diffraction biases in sonoelasticity: The acoustic impulse technique. The Journal of the Acoustical Society of America. 1999; 105:2941. [PubMed: 10335643]
6. Lerner RM, Huang SR, Parker KJ. Sonoelasticity" images derived from ultrasound signals in mechanically vibrated tissues. Ultrasound in Medicine & Biology. 1990; 16:231–9. [PubMed: 1694603]
7. Sarvazyan AP, Rudenko OV, Swanson SD, Fowlkes JB, Emelianov SY. Shear wave elasticity imaging: A new ultrasonic technology of medical diagnostics. Ultrasound Med Biol. 1998; 24:1419–1435. [PubMed: 10385964]
8. Wu Z, Taylor LS, Rubens DJ, Parker KJ. Sonoelastographic imaging of interference patterns for estimation of the shear velocity of homogeneous biomaterials. Physics in Medicine and Biology. 2004; 49:911–922. [PubMed: 15104315]
9. Ophir J, Alam SK, Garra B, Kallel F, Konofagou E, Krouskop T, Varghese T. Elastography: ultrasonic estimation and imaging of the elastic properties of tissues. Proceedings of the Institution of Mechanical Engineers Part H-Journal of Engineering in Medicine. 1999; 213:203–233.
10. Bercoff J, Tanter M, Fink M. Supersonic shear imaging: a new technique for soft tissue elasticity mapping. IEEE Transactions on Ultrasonics Ferroelectrics and Frequency Control. 2004; 51:396–409.
11. Fung, YC. Biomechanics: Mechanical Properties of Living Tissues. Springer-Verlag; 1993.
12. Vappou J, Maleke C, Konofagou EE. Quantitative viscoelastic parameters measured by harmonic motion imaging. Physics in Medicine and Biology. Jun.2009 54:3579–3594. [PubMed: 19454785]
13. Catheline S, Gennisson JL, Delon G, Fink M, Sinkus R, Abouelkaram S, Culioli J. Measurement of viscoelastic properties of homogeneous soft solid using transient elastography: An inverse problem approach. The Journal of the Acoustical Society of America. 2004; 116:3734. [PubMed: 15658723]
14. Gennisson JL, Deffieux T, Mace E, Montaldo G, Fink M, Tanter M. Viscoelastic and anisotropic mechanical properties of in vivo muscle tissue assessed by supersonic shear imaging. Ultrasound in Medicine and Biology. May.2010 36:789–801. [PubMed: 20420970]
15. Henni AH, Schmitt C, Cloutier G. Shear wave induced resonance elastography of soft heterogeneous media. Journal of Biomechanics. May.2010 43:1488–1493. [PubMed: 20171643]
16. Deffieux T, Montaldo G, Tanter M, Fink M. Shear Wave Spectroscopy for In Vivo Quantification of Human Soft Tissues Visco-Elasticity. IEEE Transactions on Medical Imaging. Mar.2009 28:313–322. [PubMed: 19244004]
17. Klatt D, Hamhaber U, Asbach P, Braun J, Sack I. Noninvasive assessment of the rheological behavior of human organs using multifrequency MR elastography: a study of brain and liver viscoelasticity. Physics in Medicine and Biology. Dec.2007 52:7281–7294. [PubMed: 18065839]
18. Kruse SA, Smith JA, Lawrence AJ, Dresner MA, Manduca A, Greenleaf JF, Ehman RL. Tissue characterization using magnetic resonance elastography: preliminary results. Physics in Medicine and Biology. Jun.2000 45:1579–1590. [PubMed: 10870712]
19. Chen S, Fatemi M, Greenleaf JF. Quantifying elasticity and viscosity from measurement of shear wave speed dispersion. The Journal of the Acoustical Society of America. 2004; 115:2781. [PubMed: 15237800]
20. Chen S, Urban M, Pislaru C, Kinnick R, Yi Z, Aiping Y, Greenleaf J. Shearwave dispersion ultrasound vibrometry (SDUV) for measuring tissue elasticity and viscosity. IEEE Transactions on Ultrasonics Ferroelectrics and Frequency Control. 2009; 56:55–62.
21. Sinkus R, Tanter M, Xydeas T, Catheline S, Bercoff J, Fink M. Viscoelastic shear properties of in vivo breast lesions measured by MR elastography. Magnetic Resonance Imaging. Feb.2005 23:159–165. [PubMed: 15833607]
22. Chen S, Fatemi M, Greenleaf JF. Remote measurement of material properties from radiation force induced vibration of an embedded sphere. J Acoust Soc Amer. 2002; 112:884–889. [PubMed: 12243175]

23. Aglyamov SR, Karpiouk AB, Ilinskii YA, Zabolotskaya EA, Emelianov SY. Motion of a solid sphere in a viscoelastic medium in response to applied acoustic radiation force: Theoretical analysis and experimental verification. Journal of the Acoustical Society of America. Oct.2007 122:1927–1936. [PubMed: 17902829]
24. Karpiouk AB, Aglyamov SR, Ilinskii YA, Zabolotskaya EA, Emelianov SY. Assessment of Shear Modulus of Tissue Using Ultrasound Radiation Force Acting on a Spherical Acoustic Inhomogeneity. IEEE Transactions on Ultrasonics Ferroelectrics and Frequency Control. Nov. 2009 56:2380–2387.
25. Hamhaber U, Grieshaber VA, Nagel JH, Klose U. Comparison of quantitative shear wave MR-elastography with mechanical compression tests. Magnetic Resonance in Medicine. Jan.2003 49:71–77. [PubMed: 12509821]
26. Ringleb SI, Chen QS, Lake DS, Manduca A, Ehman RL, An KN. Quantitative shear wave magnetic resonance elastography: Comparison to a dynamic shear material test. Magnetic Resonance in Medicine. May.2005 53:1197–1201. [PubMed: 15844144]
27. Zhai L, Palmeri ML, Bouchard RR, Nightingale RW, Nightingale KR. An integrated indenter-ARFI imaging system for tissue stiffness quantification. Ultrasonic Imaging. 2008; 30:95–111. [PubMed: 18939611]
28. Fromageau J, Gennisson JL, Schmitt C, Maurice RL, Mongrain R, Cloutier G. Estimation of polyvinyl alcohol cryogel mechanical properties with four ultrasound elastography methods and comparison with gold standard testings. IEEE Transactions on Ultrasonics Ferroelectrics and Frequency Control. Mar.2007 54:498–509.
29. Oudry J, Bastard C, Miette V, Willinger R, Sandrin L. Copolymer-in-oil phantom materials for elastography. Ultrasound in Medicine and Biology. Jul.2009 35:1185–1197. [PubMed: 19427100]
30. Oudry J, Vappou J, Choquet P, Willinger R, Sandrin L, Constantinesco A. Ultrasound-based transient elastography compared to magnetic resonance elastography in soft tissue-mimicking gels. Physics in Medicine and Biology. Nov.2009 54:6979–6990. [PubMed: 19887718]
31. Oudry J, Chen J, Glaser KJ, Miette V, Sandrin L, Ehman RL. Cross-Validation of Magnetic Resonance Elastography and Ultrasound-Based Transient Elastography: A Preliminary Phantom Study. Journal of Magnetic Resonance Imaging. Nov.2009 30:1145–1150. [PubMed: 19856447]
32. Al-ja'afreh T, Zweiri Y, Seneviratne L, Althoefer K. A new soft-tissue indentation model for estimating circular indenter 'force-displacement' characteristics. Proceedings of the Institution of Mechanical Engineers Part H Journal of Engineering in Medicine. 2008; 222:805–815.
33. Paillermattei C, Bec S, Zahouani H. In vivo measurements of the elastic mechanical properties of human skin by indentation tests. Medical Engineering & Physics. 2008; 30:599–606. [PubMed: 17869160]
34. Carter FJ, Frank TG, McLean D, Cuschieri A. Measurements and modeling of the compliance of human and porcine organ. Med Image Anal. 2001; 5:231–236. [PubMed: 11731303]
35. Miller K, Chinzei K, Orssengo G, Bednarz P. Mechanical properties of brain tissue : Experiment and computer simulation. J Biomech. 2000; 33:1369–1376. [PubMed: 10940395]
36. Kim, J.; Srinivasan, MA. Medical Image Computing and Computer-Assisted Intervention - MICCAI 2005. Vol. 3750. Springer-Verlag; 2005. Characterization of Viscoelastic Soft Tissue Properties from In Vivo Animal Experiments and Inverse FE Parameter Estimation; p. 599-606.
37. Tay BK, Kim J, Srinivasan MA. In Vivo Mechanical Behavior of Intra-abdominal Organs. IEEE Transactions on Biomedical Engineering. 2006; 53:2129–2138. [PubMed: 17073317]
38. Schwartz JM, Denninger M, Rancourt D, Moisan C, Laurendeau D. Modeling liver tissue properties using a on-linear viscoelastic model for surgery simulation. Med Imag Anal. 2005; 9:103–112.
39. Samur E, Sedef M, Basdogan C, Avtan L, Duzgun O. A robotic indenter for minimally invasive measurement and characterization of soft tissue response. Medical Image Analysis. 2007; 11:361–373. [PubMed: 17509927]
40. Ahn B, Kim J. Measurement and characterization of soft tissue behavior with surface deformation and force response under large deformations. Medical Image Analysis. 14:138–148. [PubMed: 19948423]

41. Hayes WC, Herrmann G, Mockros LF, Keer LM. A mathematical analysis for indentation tests of articular cartilage. J Biomech. 1972; 5:541–551. [PubMed: 4667277]
42. Urban MW, Chen S, Greenleaf J. Harmonic motion detection in a vibrating scattering medium. IEEE Transactions on Ultrasonics Ferroelectrics and Frequency Control. 2008; 55:1956–1974.
43. Hasegawa H, Kanai H. Improving accuracy in estimation of artery-wall displacement by referring to center frequency of RF echo. IEEE Transactions on Ultrasonics Ferroelectrics and Frequency Control. 2006; 53:52–63.
44. Morse, PM.; Ingard, KU. Theoretical Acoustics. Princeton, NJ: Princeton University Press; 1968.
45. Hayes, MH. Digital Signal Processing. McGraw-Hill; 1999.
46. Walker F, Trahey E. A fundamental limit on delay estimation using partially correlated speckle signals. IEEE Trans Ultrason, Ferroelect, Freq Contr. 1995; 42:301–308.
47. Zheng Y, Chen S, Tan W, Kinnick R, Greenleaf JF. Detection of tissue harmonic motion induced by ultrasonic radiation force using pulse-echo ultrasound and Kalman filter. IEEE Transactions on Ultrasonics Ferroelectrics and Frequency Control. 2007; 54:290–300.
48. Amador, C.; Urban, M.; Warner, L.; Greenleaf, J. Measurements of swine renal cortex shear elasticity and viscosity with Shearwave Dispersion Ultrasound Vibrometry. International Ultrasonics Symposium; Rome, Italy. 2009. p. 491-494.
49. Urban MW, Chen SG, Greenleaf JF. Error in Estimates of Tissue Material Properties from Shear Wave Dispersion Ultrasound Vibrometry. IEEE Transactions on Ultrasonics Ferroelectrics and Frequency Control. Apr.2009 56:748–758.
50. Nenadic, I.; Urban, MW.; Greenlea, JF. Ex vivo measurements of mechanical properties of myocardium using Lamb and Rayleigh wave dispersion velocities. IEEE International Ultrasonics Symposium (IUS); Rome, Italy. 2009. p. 2785-2788.

## Biographies

**Carolina Amador** (IEEE/S’09) was born in Medellin, Colombia on April 14, 1984. She received the B.S. degree in biomedical engineering at Escuela de Ingenieria de Antioquia, Medellin, Colombia, in 2006. She is currently a graduate student in the biomedical engineering PhD program at the Mayo Clinic College of Medicine in Rochester, MN, USA. She has been a visiting undergraduate student at the Biomedical Imaging Resource at Mayo Clinic, Rochester, MN, USA. Her research interest is noninvasive evaluation of mechanical properties of soft tissue.

**Matthew W. Urban** (IEEE/S’02, M’07) was born in Sioux Falls, SD in on February 25, 1980. He received the B.S. degree in electrical engineering at South Dakota State University, Brookings, SD in 2002 and the Ph.D. in biomedical engineering at the Mayo Clinic College of Medicine in Rochester, MN in 2007. He is currently an Assistant Professor

in the Department of Biomedical Engineering, Mayo Clinic College of Medicine. He has been a Summer Undergraduate Fellow at the Mayo Clinic Biomechanics laboratory. His current research interests are ultrasonic signal and image processing, vibro-acoustography, and vibrometry applications. Dr. Urban is a member of Eta Kappa Nu, Tau Beta Pi, IEEE, and the Acoustical Society of America.

**Shigao Chen** (M'02) received the B.S. and M.S. degrees in biomedical engineering from Tsinghua University, China, in 1995 and 1997 respectively, and the Ph.D. degree in biomedical imaging from the Mayo Graduate School, Rochester, MN in 2002. He is currently Assistant Professor of Mayo Graduate School, and Associate Consultant, Department of Biomedical Engineering, Mayo Clinic College of Medicine. His research interest is noninvasive quantification of viscoelastic properties of soft tissue using ultrasound.

**Qingshan Chen** received his M.S. in Biomedical Engineering in Memphis, TN in 2001.

He is a research engineer at the Orthopedic Biomechanics Laboratory at the Mayo Clinic in Rochester, MN, and Assistant Professor of Bioengineering, Mayo Medical School. He has co-authored more than 50 scientific articles and book chapters, most being in peer-reviewed journals.

Mr. Chen's research interests include tissue biomechanics, biomaterials, orthopedics and magnetic resonance elastography. He has received several awards from various societies.

**Kai-Nan An** received his Ph.D. in mechanical engineering and applied mechanics in 1975 from Lehigh University in Bethlehem, PA.

He is the Director (1993-present) of the Orthopedic Biomechanics Laboratory at the Mayo Clinic in Rochester, MN, and Professor of Bioengineering, Mayo Medical School. He was named the John and Posy Krehbiel Professor of Orthopedics, Mayo Medical School, in 1993. He has co-authored more than 700 scientific articles and book chapters, most being in

peer-reviewed journals. Dr. An's research interests include biomechanics, biomaterials, orthopedics and rehabilitation. He has received several awards from various societies, including being named as a Fellow of the ASME in 2007. He is a founding member of the American Institute for Medical and Biological Engineering, and serves as advisor to graduate students and research fellows, as well as various medical and engineering organizations.

**James F. Greenleaf** (M'73–SM'84–F'88) was born in Salt Lake City, UT, on February 10, 1942. He received the B.S. degree in electrical engineering from the University of Utah, Salt Lake City, in 1964, the M.S. degree in engineering science from Purdue University, Lafayette, IN, in 1968, and the Ph.D. degree in engineering science from the Mayo Graduate School of Medicine, Rochester, MN, and Purdue University in 1970. He is currently Professor of Biomedical Engineering and Associate Professor of Medicine, Mayo Medical School, and Consultant, Department of Physiology, Biophysics, and Cardiovascular Disease and Medicine, Mayo Foundation.

He has served on the IEEE Technical Committee for the Ultrasonics Symposium for seven years. He served on the IEEE Ultrasonics, Ferroelectrics, and Frequency Control Society (UFFC-S) Subcommittee on Ultrasonics in Medicine/IEEE Measurement Guide Editors, and on the IEEE Medical Ultrasound Committee. Doctor Greenleaf was President of the UFFC-S in 1991 and Vice President for Ultrasonics in 1992 to 2003.

Dr. Greenleaf has 12 patents and is a recipient of the 1986 J. Holmes Pioneer Award and the 1998 William J. Fry Memorial Lecture Award from the American Institute of Ultrasound in Medicine, and is a Fellow of IEEE, American Institute of Ultrasound in Medicine, and American Institute for Medical and Biological Engineering. Dr. Greenleaf was the Distinguished Lecturer for IEEE Ultrasonics, Ferroelectrics, and Frequency Control Society (1990/1991). His special field of interest is ultrasonic biomedical science, and he has published more than 237 peer-reviewed articles and edited or authored five books in the field.

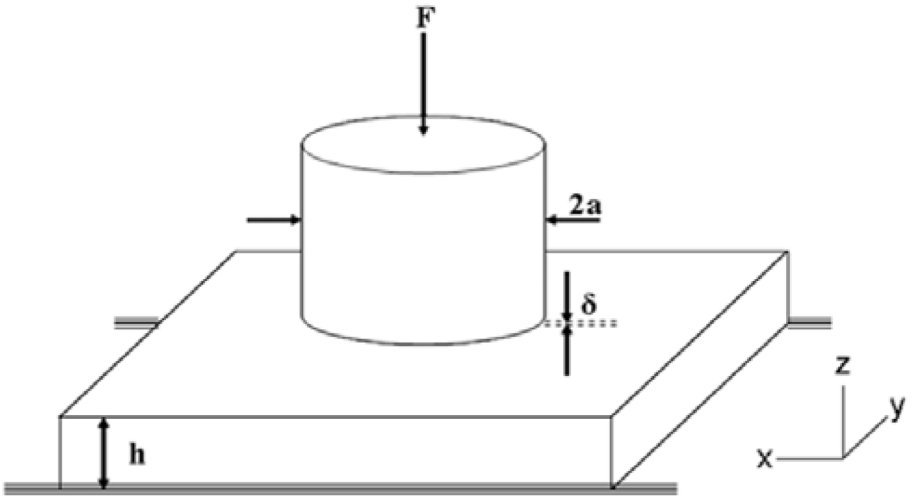


**Fig. 1.**
Experimental set up, where *F* is the indentation force, *Δ* is the indentation depth, *a* is the indenter radius, and *h* is the material thickness.

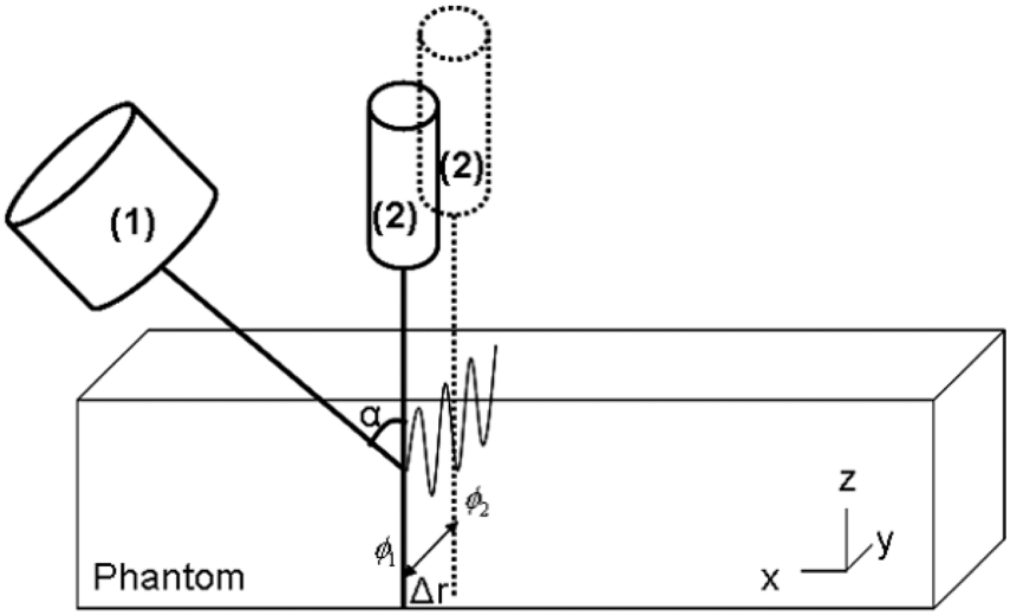


**Fig. 2.**

Illustration of the experimental set up. SDUV applies a localized force generated by a 'Push Transducer' (1) coupled to the phantom, transmitting repeated tonebursts of ultrasound. A separated transducer acts as the detector, 'Detect Transducer' (2).

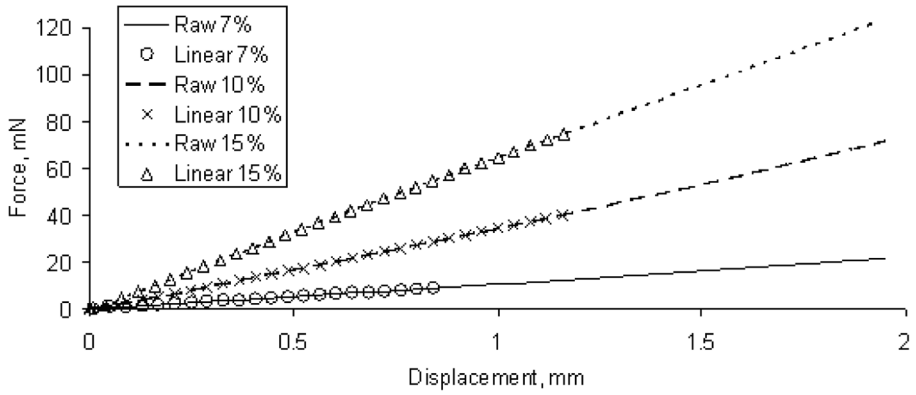


**Fig. 3.**

Force-displacement data for one sample of each gelatin phantom (Sample type 1, refer to Table I). The three symbols represent the linear region for the three gelatin phantoms. The three line types represent the raw data for the three gelatin phantoms.

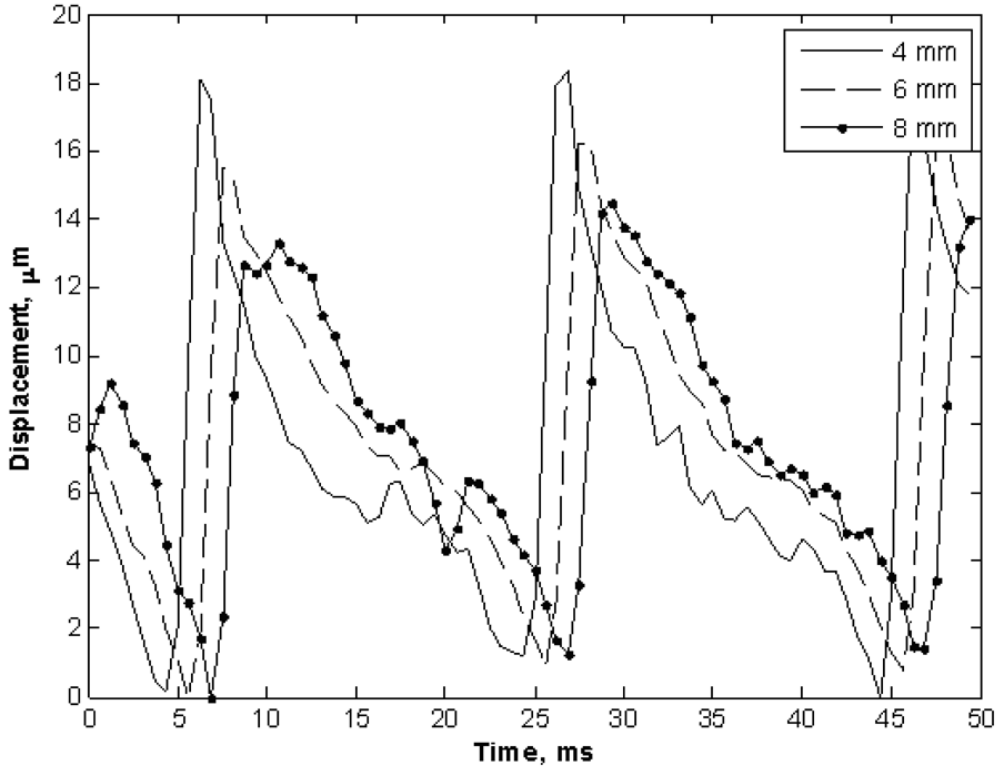


**Fig. 4.**

Displacement amplitude estimates over 50 ms for 7% gelatin phantom. The three symbols represent three sets of the measured amplitude for 4, 6 and 8 mm away from the vibration center.

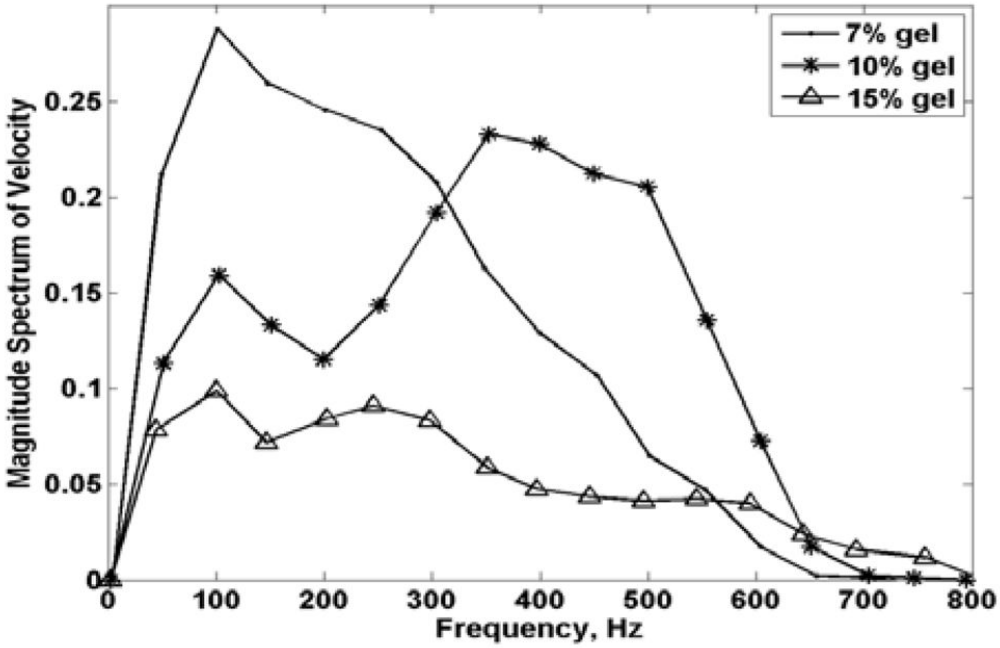


**Fig. 5.**
Magnitude spectra of the velocity signals over 200 msec. The three symbols represent 7, 10 and 15% gelatin phantoms.

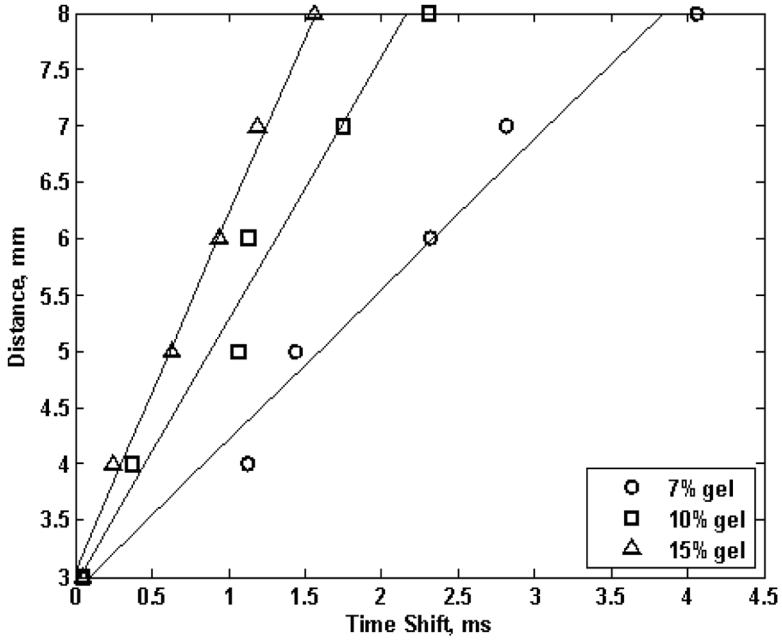


**Fig. 6.**

Time shift estimates for the gelatin phantoms over 3 to 8 mm away from the vibration center. The three symbols represent 7, 10 and 15% gelatin phantoms. The solid line represents linear regression.

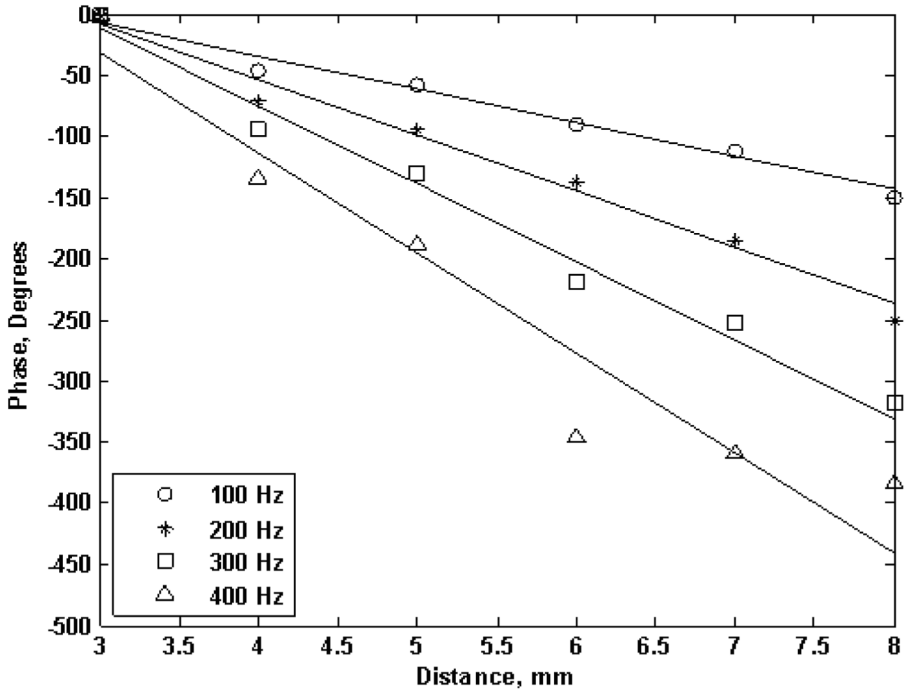


**Fig. 7.**

Phase estimates for the 7% gelatin phantom over 3 to 8 mm away from the vibration center. The four symbols represent four sets of estimated phase changes over the distance for four vibrations with frequencies from 100 Hz to 400 Hz. The solid line represents linear regression.

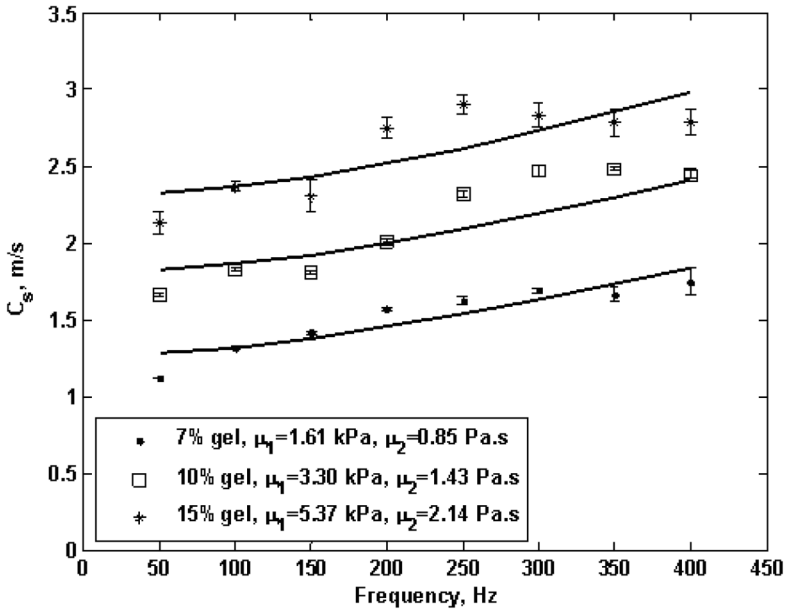


**Fig. 8.**

Shear wave speed measured from 50 Hz to 400 Hz. The three symbols represent 7, 10 and 15% gelatin phantoms. The solid lines are fits from the Voigt dispersion model, which gives estimates of shear elastic modulus ($\mu_1$) and viscosity ($\mu_2$) shown at the bottom of this figure.

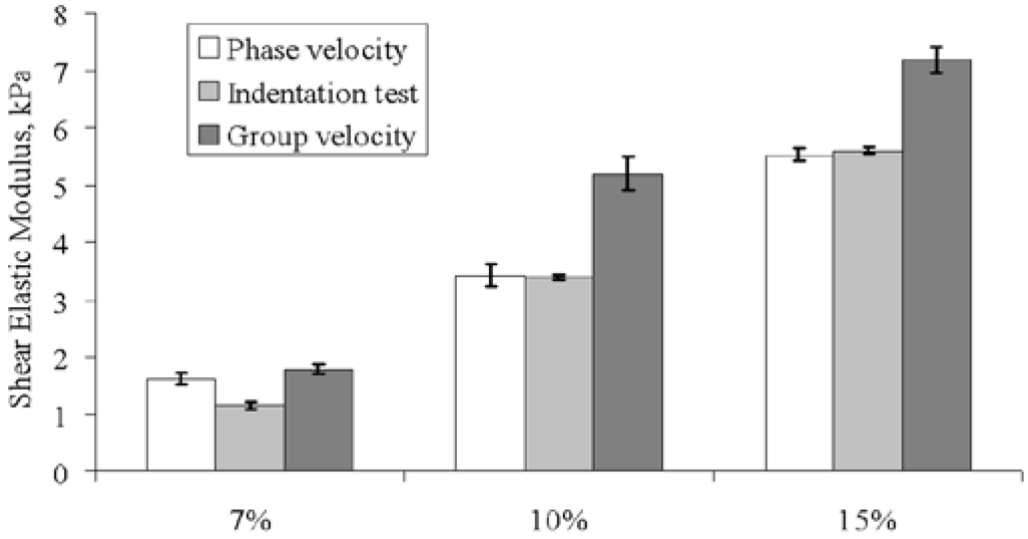


**Fig. 9.**
Shear elastic modulus comparison between phase velocity, indentation test and group velocity. Mean ± SD, n=4

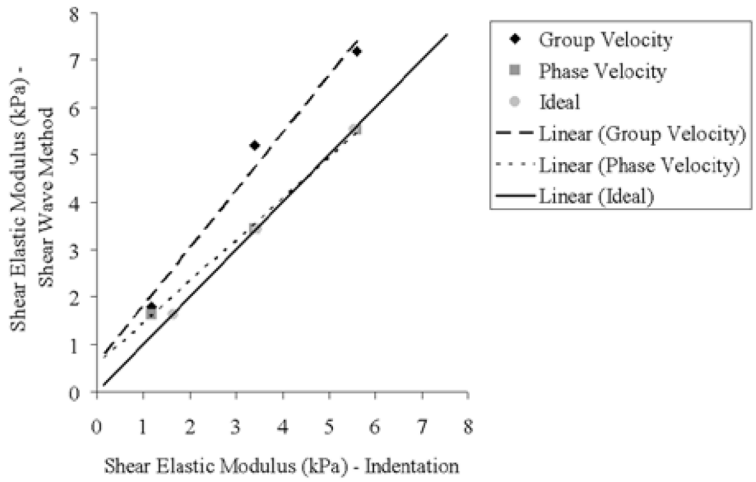


**Fig. 10.**

Linear correlation comparing indentation test with group velocity (diamonds and dashed line) and SDUV phase velocity (squares and dotted line). The continuous line represents an ideal correlation.

**Table I**

Sample characterization for mechanical test. Four samples of each type were made.

| **7% gelatin phantom** | | |
|---|---|---|
| **Sample type** | **Thickness (mm)** | **Diameter (mm)** |
| 1 | 7.98 | 35 |
| 2 | 17.44 | 35.3 |
| 3 | 7.98 | 13.8 |
| 10% gelatin phantom | | |
| Sample type | Thickness (mm) | Diameter (mm) |
| 1 | 7.88 | 35 |
| 2 | 17 | 35.3 |
| 3 | 7.88 | 13.8 |
| 15% gelatin phantom | | |
| Sample type | Thickness (mm) | Diameter (mm) |
| 1 | 7.3 | 35 |
| 2 | 19 | 35.3 |
| 3 | 7.3 | 13.8 |

**Table II**

Shear elastic modulus (kPa) for different sample diameter (d), indenter diameter (2a) and sample thickness.

| 7% gelatin phantom | | | | |
|---|---|---|---|---|
| Thickness (mm) | 2a= 2 mm | 2a= 3 mm | 2a= 2 mm | 2a= 3 mm |
| | D= 35 mm | D= 35 mm | D= 13.8 mm | D= 13.8 mm |
| 7.98 | 1.35 ± 0.06 | 1.36 ± 0.01 | 1.29 ± 0.19 | 1.22 ± 0.20 |
| 17.44 | 1.16 ± 0.01 | 1.29 ± 0.04 | - | - |
| 10% gelatin phantom | | | | |
| Thickness (mm) | 2a= 2 mm | 2a= 3 mm | 2a= 2 mm | 2a= 3 mm |
| | D= 35 mm | D= 35 mm | D= 13.8 mm | D= 13.8 mm |
| 7.88 | 3.65 ± 0.21 | 3.63 ± 0.14 | 3.54 ± 0.09 | 3.51 ± 0.12 |
| 17 | 3.40 ± 0.05 | 3.28 ± 0.09 | - | - |
| 15% gelatin phantom | | | | |
| Thickness (mm) | 2a= 2 mm | 2a= 3 mm | 2a= 2 mm | 2a= 3 mm |
| | D= 35 mm | D= 35 mm | D= 13.8 mm | D= 13.8 mm |
| 7.3 | 4.68 ± 0.03 | 4.67 ± 0.1 | 4.76 ± 0.1 | 4.63 ± 0.05 |
| 19 | 5.60 ± 0.06 | 5.00 ± 0.01 | - | - |

mean ± SD, n = 4

**Table III**

Group velocity, phase velocity evaluated at center of gravity and phase velocity evaluated at center frequency

| | 7% gelatin phantom | 10% gelatin phantom | 15% gelatin phantom |
|---|---|---|---|
| Group Velocity, $c_g$ | 1.33 m/s | 2.35 m/s | 3.15 m/s |
| Phase Velocity at $\omega_c$, $c_s(\omega_c)$ | 1.57 m/s | 2.49 m/s | 2.83 m/s |
| Phase Velocity at $\omega_p$, $c_s(\omega_p)$ | 1.32 m/s | 2.49 m/s | 2.38 m/s |